Integration of Zero Crossing Method in a Non-Uniform Sampling System using Optical Feedback Interferometry

Hajira S Bazaz, Mohaimen M Fatimah, Layba Asim, Usman Zabit, Olivier D Bernal

Integration of Zero Crossing Method in a Non-Uniform Sampling System using Optical Feedback Interferometry

Hajira S. Bazaz[1], Mohaimen M. Fatimah[1], Layba Asim[1], Usman Zabit[1], and Olivier D. Bernal[2],

[1]Department of Electrical Engineering, National University of Sciences and Technology (NUST), Islamabad, Pakistan

[2] LAAS-CNRS, Université de Toulouse, CNRS, INP, Toulouse, France

DOI: 10.1109/JSEN.2023.3275702

***Abstract*— In this paper, a zero-crossings based method is proposed to improve the displacement sensing performance of non-uniform sampling (NUS) theory based use of optical feedback interferometry (OFI) under moderate optical feedback regime. The incorporation of zero-crossings as phase quantization levels allows doubling the samples for subsequent interpolation, without using any dithering scheme. When compared to the simple dither-free NUS method, the proposed method yields an overall improvement in RMS error over a wide range of target motion amplitudes and frequencies, with maximum improvement at low amplitudes. Experimentally, an improvement of up to 87% is obtained in precision as compared to simple NUS system for an OFI sensor with laser wavelength of 785 nm.**

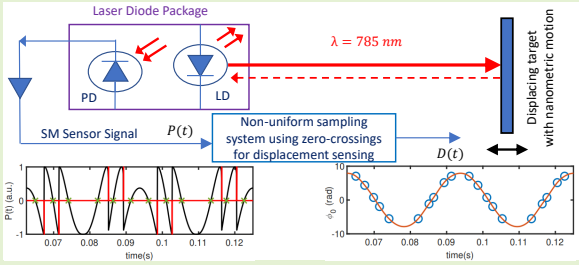

***Index Terms*— Non-uniform sampling, Optical feedback interferometry, Self-mixing, Zero crossings, Displacement measurement**

I. Introduction

OPTICAL feedback interferometry (OFI) is a well-known method for displacement measurement using a laser diode (LD) as it benefits from its inherent self-aligned property as well as its low-cost [1], [2]. As a result, OFI has been applied in a wide range of sensing applications, including the measurement of distance [3], displacement [4], velocity [5], acceleration [6], flow [7], temperature [8], strain [9] vibration [10] and bio-sensing [11].

To retrieve the displacement information embedded in both the amplitude modulation (AM) and frequency modulation (FM) channel of OFI signals [12], different techniques have been developed over the years from basic fringe counting [13] to more advanced ones such as fringe-locking [14], fringe duplication [15] and phase unwrapping [16]–[19].

An open-loop approach based on the inherent non-uniform sampling (NUS) capability of the SM interferometer was recently proposed to recover sub-$\lambda_0/2$ displacement with precision down to the nanometer in the moderate feedback regime [4], [20] which corresponds to an optical feedback factor $C \in [1, 4.6]$. In this optical regime where the fringes are sawtooth like, optical feedback interferometers behave as an inherent NUS system with its own embedded phase level crossing detector. Consequently, it allows to perform compressed sensing as the displacement can be reconstructed from the information related to the fringe disconitnuity locations only. The main limitation of the NUS method [4] is its degraded performance when the remote target's displacement amplitude is such that there are not sufficient number of fringes needed to satisfy Nyquist's sampling criterion [4]. So, when remote displacement amplitude becomes comparable to $\lambda_0/2$ then NUS based interpolation becomes imprecise. This limitation was addressed in [4] by using dithering techniques to increase the number of sampling events (or number of fringes). For example, [4] added a mechanical dither by vibrating the LD via an external shaker. However, this resulted in a bulky laser-shaker setup with a limited system bandwidth. In another work [20], phase dithering was used to introduce additional fringes by modulating the LD driving current instead of using an external shaker. Note that in both the cases [4], [20], the effect of dithering had to be removed before actual remote target's motion could be measured.

This paper presents an alternate solution to dithering for improving the resolution and precision of the NUS-based approach. The proposed method incorporates the zero-crossings (ZC) of the OFI signal in addition to the fringe discontinuities to double the samples for interpolation. The aim is to increase the precision of recovered displacement around its local maxima and minima, especially when displacement amplitudes are comparable to $\lambda_0/2$.

The rest of the paper is organized as follows. Section

II provides a brief overview of the fundamentals of OFI and the theory behind NUS based OFI. Section III presents the methodology of the proposed zero-crossings based NUS method. In Section IV, the proposed method is tested on simulated signals and parametric sweeps have been presented to show its performance. Experimental results are presented in Section V, followed by Discussion and Conclusion.

II. OFI and Non-Uniform Sampling - Review

A. OFI Overview

The basic principles of OFI have been thoroughly established, such as in [1]. A brief overview is as follows.

OFI involves directing a laser beam, with wavelength λ_0, at a remote target vibrating with a displacement $D(t)$, which then back-scatters the beam back into the laser cavity. The electrical and optical characteristics of the laser cavity are altered as a result of this feedback. The modulated OOP signal $P(t)$ is given in [1] as

$$P(t) = P_0[1 + m\cos(\phi_F(t))] \tag{1}$$

where P_0 is the emitted optical power under free-running conditions, m is the modulation index, and $\phi_F(t)$ is the laser phase with optical feedback. The signal $P_N(t)$ is the normalized OOP, given by

$$P_N(t) = \cos(\phi_F(t)) \tag{2}$$

$\phi_F(t)$ is related to the laser phase without feedback $\phi_0(t)$ through the Lang-Kobayashi excess phase equation [21], given as

$$\phi_0(t) = \phi_F(t) + C\sin(\phi_F(t) + \theta) \tag{3}$$

where C is the optical feedback coupling factor [22] or Acket's parameter [23], $\theta = \arctan(\alpha)$ and α is the linewidth enhancement factor or Henry's factor [24]. These principal equations allow measuring $D(t)$ using the detected OOP signal since $\phi_0(t)$ can be expressed as

$$\phi_0(t) = \frac{4\pi}{\lambda_0}\, D(t) \tag{4}$$

B. Overview of OFI Non-Uniform Sampling

It has been shown in [4] that an SM interferometer can be considered as an inherent NUS system with its own built-in phase-level crossing detector. The phase quantization levels (PQLs) are represented by $\phi_{0_D}(k)$ that occur at the fringe discontinuity points of the OOP signal. We refer to $\phi_{0_{D,R}}(k)$ and $\phi_{0_{D,F}}(k)$ as the phase ϕ_{0_D} when it is increasing and decreasing, respectively. In terms of ϕ_F, the PQLs are completely defined in [25] as

$$\phi_{F_{D,R}}(k) = k\pi - \theta + \beta \tag{5}$$

$$\phi_{F_{D,F}}(k) = (k+2)\pi - \theta - \beta \tag{6}$$

where k is an even integer and $\beta = \arctan\left(-\frac{1}{C}\right)$. Substituting (5) and (6) in (3) gives us the PQLs in terms of ϕ_0:

$$\phi_{0_{D,R}}(k) = k\pi - \theta + \beta + \sqrt{C^2 - 1} \tag{7}$$

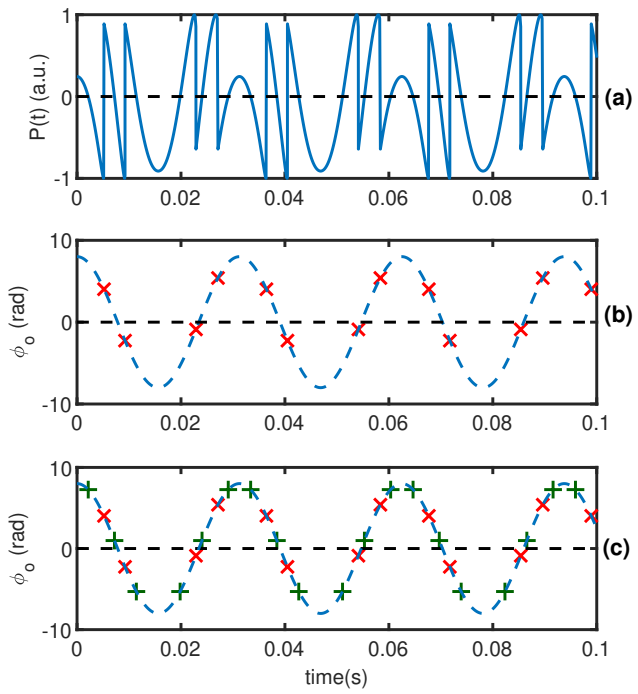

Fig. 1. (a) Simulated normalized self-mixing signal obtained for a sinusoidal displacement with amplitude 0.5 μm at 32 Hz using a laser wavelength λ_0 = 785 nm, C = 2 and α = 5, and corresponding interpolated phase ϕ_0 (dashed line): (b) with only the fringe discontinuities (red markers) detected, and (c) with both discontinuities and zero-crossings (green markers) detected.

$$\phi_{0_{D,F}}(k) = (k+2)\pi - \theta - \beta - \sqrt{C^2 - 1} \tag{8}$$

It has been shown in [4] that the values of ϕ_0 at rising phase differ from those at falling phase by an amount, denoted as $\Delta\phi$, given by

$$\Delta\phi = \beta + \sqrt{C^2 - 1} - \pi \tag{9}$$

It was demonstrated in [26] that C can be retrieved by estimating this phase level difference $\Delta\Phi$. Thus, the simple NUS based approach described in [4] interpolates just these discontinuity points to recover the phase signal $\phi_0(t)$. This interpolated signal is then used in (4) to recover $D(t)$, as shown in Fig. 1 (b).

It was discussed in [4] that the existing NUS method does not provide high measurement precision when the remote target motion is of low amplitude because the corresponding OFI signal has too few fringe discontinuity points available. The concept of dithering (via laser diode current modulation or mechanical dithering) [4], [20] was then used to increase the number of samples (by increasing the number of fringes) so that interpolation performance could be increased. The effect of introduced dithering then had to be subtracted before actual target motion could be recovered, as schematized in Fig. 2.

III. Proposed Zero-Crossing based NUS Method

In this paper, we propose to incorporate zero-crossings of the OFI signal in addition to the previously used fringe

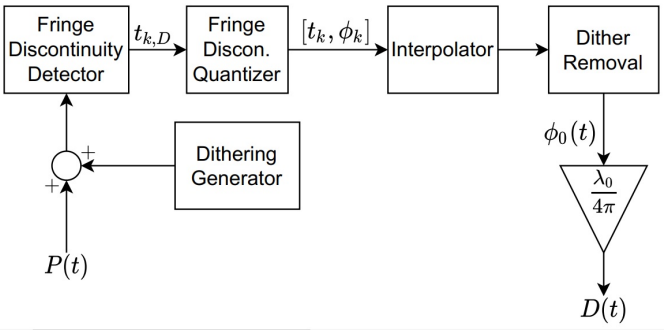

Fig. 2. Schematic block diagram of OFI based non-uniform sampling (NUS) system using dithering, reported in [4].

discontinuities in the time-phase pairs. This results in doubling the number of detected samples/events so that better interpolation performance can be achieved for the same target motion without resorting to the use of dithering.

To achieve this objective, we need to first derive the laser phase values ϕ_{F_Z} and ϕ_{0_Z} at the zero-crossing points in a given moderate feedback regime OFI signal.

As per (2), the OFI signal, or OOP, is zero whenever

$$\phi_{F_Z}(k) = \frac{(2k-1)\pi}{2} \tag{10}$$

where k is an even integer. Incorporating (10) into (3), we get the phase ϕ_{0_Z} at zero-crossings for $C > 1$:

$$\phi_{0_Z}(k) = \frac{(2k-1)\,\pi}{2} - C\cos(\theta) \tag{11}$$

We then find the phase difference between the zero-crossings as in (11) and discontinuities as in (7) and (8) for increasing phase and decreasing phase, respectively:

$$\begin{aligned}\Delta\phi_{DZ,R} &= \phi_{0_D,R}(k) - \phi_{0_Z}(k) \\ &= \frac{\pi}{2} - \theta + \beta + C\cos(\theta) + \sqrt{C^2-1}\end{aligned} \tag{12}$$

$$\begin{aligned}\Delta\phi_{DZ,F} &= \phi_{0_D,F}(k) - \phi_{0_Z}(k) \\ &= \frac{5\pi}{2} - \theta - \beta + C\cos(\theta) - \sqrt{C^2-1}\end{aligned} \tag{13}$$

Note that C is needed in the derived expressions. Here, the C estimation method proposed in [26] is used, as shown in Fig. 3. The impact of error in C estimation on the reconstructed displacement has been analyzed in the following section.

Expressions (12) and (13) are then used in the ZC quantizer shown in Fig. 3 to incorporate the zero-crossing time-stamps $t_{k,Z}$ provided by the zero-crossing detector. These new time-stamps are then incorporated alongside the previously obtained time-phase pairs $[t_k, \phi_k]$. This results in doubling the number of time-phase pairs $[t'_k, \phi'_k]$ as compared to the simple NUS method, as shown in Fig. 1 (c). All of these are then spline-interpolated to reconstruct the phase signal $\phi_0(t)$ which provides displacement via (4). This process is schematized in Fig. 3.

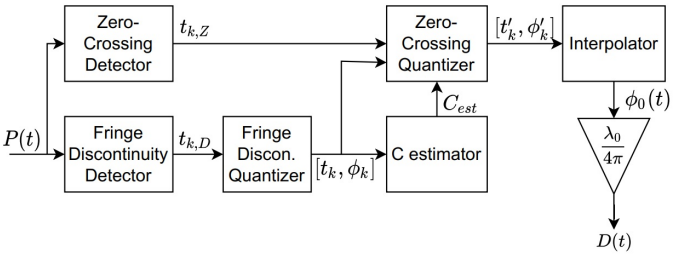

Fig. 3. Schematic block diagram of proposed zero-crossings based NUS system using OFI. C estimation uses the method reported in [26].

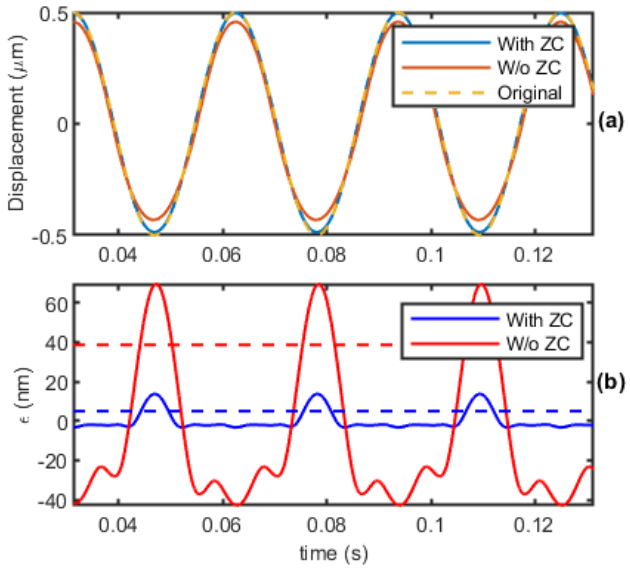

Fig. 4. Simulated results of reconstructing the displacement from an OFI signal corresponding to a harmonic motion with $\boldsymbol{A_t}$ = 0.5 µm, $\boldsymbol{f_t}$ = 32 Hz, $\boldsymbol{C}$ = 2, $\boldsymbol{\alpha}$ = 5, $\boldsymbol{\lambda_0}$ = 785 nm and $\boldsymbol{F_s}$ = **10** MHz. (a) Comparison of reference target motion (dashed line) with reconstructed displacement with- (blue line) and without-proposed zero-crossing (ZC) method (red line). (b) Corresponding error in reconstructed displacement $\boldsymbol{\epsilon}$ (unbroken line) and its RMS value (dashed line).

IV. Simulated Results

The newly derived ZC method and the simple dither-less NUS method [4] were separately applied to recover the simulated displacement of a remote target vibrating at a frequency, f_t, of 32 Hz with amplitude, A_t, of 0.5 µm such that C = 2, α = 5, λ_0 = 785 nm, and sampling frequency, denoted as F_s, is 10 MHz. Using the reference displacement, error in reconstruction, denoted as ϵ, is computed for the two methods, as plotted in Fig. 4 (b). Comparison of the two methods indicates that the new method results in a 70% reduction in root-mean-square (RMS) error, ϵ_{rms}. Also, it can be observed in Fig. 4 that the new method is most beneficial around the so-called humps of the OFI signal (or around the maxima and minima of the remote vibration), where the previous method [4] lacks samples for interpolation.

A detailed analysis of measurement performance of the proposed method, as a function of various system parameters, is now presented below.

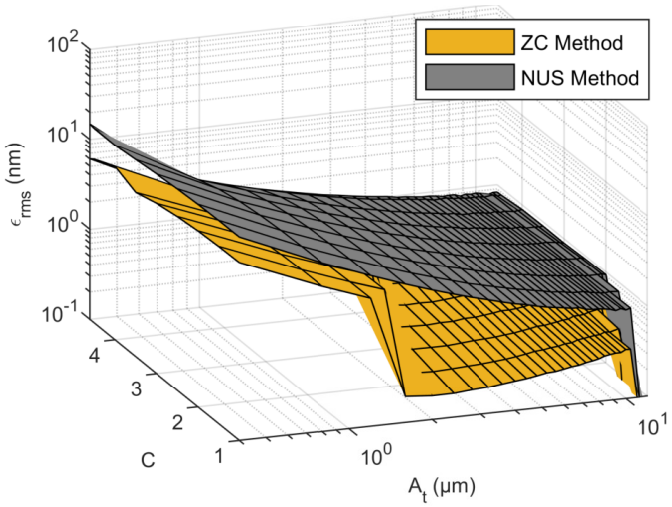

Fig. 5. Simulation based RMS Error (nm) of zero-crossing and simple NUS methods as a function of $\boldsymbol{C}$ ($\mathbf{1.0} \leq \boldsymbol{C} \leq \mathbf{4.6}$) and vibration amplitude $\boldsymbol{A_t}$ (0.4 μm $\leq \boldsymbol{A_t} \leq$ 12 μm) for $\boldsymbol{f_t}$ = 32 Hz, $\boldsymbol{F_s}$ = **10** MHz, $\boldsymbol{\lambda_0}$ = 785 nm and $\boldsymbol{\alpha}$ = 5.

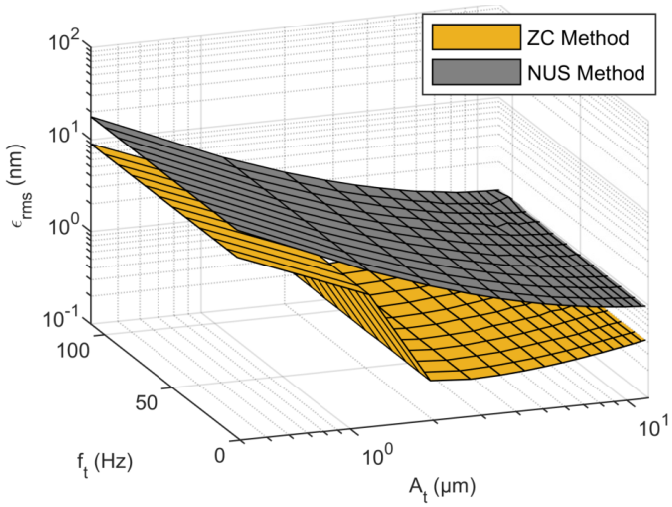

Fig. 6. Simulation based RMS Error (nm) of zero-crossing and simple NUS methods as a function of amplitude (0.4 μm $\leq \boldsymbol{A_t} \leq$ 12 μm) and frequency (2 Hz $\leq \boldsymbol{f_t} \leq$ 110 Hz) of target motion for $\boldsymbol{F_s}$ = **10** MHz, $\boldsymbol{\lambda_0}$ = 785 nm, $\boldsymbol{C}$ = 2 and $\boldsymbol{\alpha}$ = 5.

A. Effect of C, Displacement Amplitude, and Frequency

Fig. 5 presents a comparison of simulation based RMS error between the proposed ZC method and the simple NUS method [4] as a function of C and A_t. As compared to the simple NUS method, a 25% to 95% improvement in performance is observed with the ZC method for 0.4 μm $\leq A_t \leq$ 12 μm when λ_0 = 785 nm, equivalent to an OFI signal with approximately 2 to 60 fringes per cycle. A 50% reduction in ϵ_{rms} is noted when A_t = 0.4 μm, analogous to an OFI signal with approximately 2 fringes per cycle. Moreover, ϵ_{rms} as low as 0.0645 nm is obtained over the defined range when using the proposed ZC method for C = 1 and A_t = 11.2 μm.

Similarly, Fig. 6 features the simulation based ϵ_{rms} comparison as a function of A_t and f_t. Here, A_t spans 0.4 μm $\leq A_t \leq$ 12 μm while f_t ranges over 2 Hz $\leq f_t \leq$ 110 Hz. F_s = 10 MHz, while λ_0 = 785 nm, C = 2 and α = 5. Approximately 50% improvement in ϵ_{rms} is observed for the specified ranges. A maximum of 94% improvement in ϵ_{rms} is detected for A_t = 2 μm and f_t = 50 Hz. Furthermore, ϵ_{rms} varies from a minimum value of 0.0078 nm, when A_t = 13.2 μm and f_t = 10 Hz, to a maximum value of 8.95 nm, when A_t = 0.4 μm and f_t = 10 Hz while using the ZC method.

B. Effect of error in C estimation

The new ZC method requires estimation of C and α to find the phase difference between the zero-crossing and the fringe discontinuity (12, 13). So, simulations were conducted to test the robustness of the ZC method against possible errors in C and α estimations.

First, the impact of the C estimation error is analyzed. The proposed method was tested for two cases of C i.e., the original simulated OFI signal $P_{org}(t)$ has C = 1.5 and 3. The value of $\widehat{C}$, i.e. the estimated C value used in reconstruction, was varied by 2%, 5%, 10%, 20%, and 50% to recover the displacement. This was then compared with the original displacement to calculate the RMS error shown in Table I and percentage improvement as compared to the NUS method is shown in Table II. Here, the percentage improvement is defined as:

$$\%\ Imp.\ = \frac{\epsilon_{rms,\ NUS}\ -\ \epsilon_{rms,\ ZC}}{\epsilon_{rms,\ NUS}} \times 100 \qquad (14)$$

TABLE I
SIMULATION BASED RMS ERROR RESULTS OF THE PROPOSED ZC METHOD AGAINST VARIATIONS IN THE VALUE OF $\widehat{C}$ WITH α = 3 FOR A TARGET MOTION OF 0.5 μM AMPLITUDE AT 32 HZ FREQUENCY.

% Error in C	C = 1.5		C = 3.0	
	$\widehat{C}$	ϵ_{rms} (nm)	$\widehat{C}$	ϵ_{rms} (nm)
0	1.50	4.4	3.00	3.1
2	1.53	4.1	3.06	7.9
5	1.58	4.0	3.15	17.1
10	1.65	4.5	3.30	32.8
20	1.80	7.2	3.60	64.6
50	2.25	19.0	4.50	160.1

The tabulated results show that for C = 1.5 there is no significant change in RMS error for up to 20% error in estimation of C but in the case of C = 3, there is a significant change in the RMS error for even 2% error in estimation of C. It is because of the shape and hysteresis in the OFI signal. For C = 1.5 the separation between the zero-crossing and fringe discontinuity is considerable (see Fig. 7 (a)) but as the value of C increases, the inter-fringe distance decreases which results in closely detected points on the rising phase (see Fig. 7 (c)) and this causes poor interpolation of the signal (see Fig. 7 (d)). In the second case, the error is caused by the detection of a fringe and discontinuity close to the hump. It is also visible in the second case that the simple NUS method gives better results for 20% or more inaccuracy in C estimation (see Table II). Here, a negative percentage improvement indicates that the NUS method performed better than the proposed method. For

TABLE II

SIMULATION BASED PERCENTAGE IMPROVEMENT IN RMS ERROR OF THE PROPOSED ZC METHOD AS COMPARED TO THE SIMPLE NUS METHOD AS A FUNCTION OF ERROR IN $\widehat{C}$ FOR A TARGET MOTION OF 0.5 µM AMPLITUDE AT 32 HZ AND $\boldsymbol{\alpha}$ = 3.

% Error in C	C = 1.5		C = 3.0	
	$\widehat{C}$	% Imp.	$\widehat{C}$	% Imp.
0	1.50	88.8	3.00	91.7
2	1.53	89.4	3.06	78.6
5	1.58	89.8	3.15	52.6
10	1.65	88.5	3.30	4.8
20	1.80	81.1	3.60	-106.2
50	2.25	48.3	4.50	-588.7

example, this occurs when C value is large and a large error in C estimation also occurs. This happens due to the fact that for a large value of C, the distance between the ZC and the discontinuity is small and therefore any mis-estimation of C can have a higher impact on the reconstructed displacement. Based on Table II), it appears that an accuracy of up to 5% in C estimation should be sufficient to achieve high measurement precision with the proposed ZC method as compared to the NUS method.

C. Effect of error in α estimation

Similarly, tests were conducted to see the effect on RMS error in case there is error in estimation of α. The original OFI signal has α = 3. RMS error was calculated after using different values of $\widehat{\alpha}$, reported in Table III. Small inaccuracy in α does not cause much change in RMS error but large inaccuracy in α causes significant change in RMS error. Hence, for better measurement performance, accurate estimation of α is desired.

TABLE III

SIMULATION BASED RMS ERROR RESULTS AND PERCENTAGE IMPROVEMENT OF THE PROPOSED ZC METHOD AS COMPARED TO THE SIMPLE NUS METHOD AS A FUNCTION OF ERROR IN $\widehat{\boldsymbol{\alpha}}$ FOR A TARGET MOTION OF 0.5 µM AMPLITUDE AT 32 HZ WITH $\boldsymbol{C}$ = 1.5 AND $\boldsymbol{\alpha}$ = 3.

$\widehat{\alpha}$	ϵ_{rms} (nm)	% Imp.
3.0	4.4	88.8
3.3	7.0	82.0
3.6	9.5	75.5
4.0	12.4	68.0
5.0	17.9	53.9
6.0	21.7	44.2
7.0	24.4	37.1

D. Effect of time-varying C

A practical issue that arises in OFI is the occurrence of speckle which manifests itself as a time-varying C such as caused by variation in roughness of the remote target surface [27]. For the proposed ZC method to perform well in a real-world scenario, it needs to be robust to possible variations in C due to speckle. So, simulations were conducted for a 0.4 µm, 32 Hz displacement signal with λ_0 = 785 nm and α = 5 such

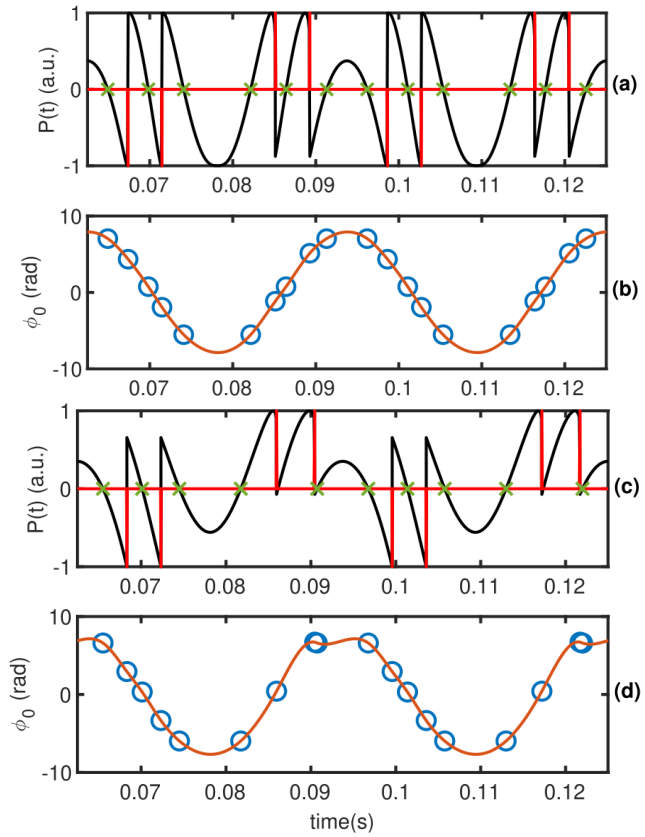

Fig. 7. Effect of error in $\boldsymbol{C}$ estimation on ZC method when $\boldsymbol{A_t}$ = 0.5 µm, and $\boldsymbol{f_t}$ = 32 Hz: (a) detected zero-crossings (green crosses) and fringe discontinuities (red vertical lines) on simulated OFI signal when original $\boldsymbol{C}$ = 1.5 and corresponding (b) interpolated phase $\boldsymbol{\phi_o}$ based on all detections (blue circles) in case there is 10% error in estimated $\boldsymbol{C}$ value i.e. $\widehat{\boldsymbol{C}}$ = 1.65. (c) OFI signal when original $\boldsymbol{C}$ = 3 and corresponding (d) interpolated phase $\boldsymbol{\phi_o}$ with 10% error in estimated $\boldsymbol{C}$ value i.e. $\widehat{\boldsymbol{C}}$ = 3.3.

that C is varied by 20% in a sinusoidal manner with a mean value of C, denoted as C_m, of 2 by using the model reported in [28] (see Fig. 8 (a)). The corresponding ZC method based recovered displacement signal in Fig. 8 (b) has a 75% lower RMS error as compared to the simple NUS method [4].

It is observed in Table IV that this improvement in reconstruction is most significant where A_t is small and comparable to $\lambda_0/2$. For higher A_t values, the simple NUS method performs better.

E. Effect of noise

The determination of the ZC events is affected by noise, thereby limiting the achievable performances by the proposed method as any quantization level uncertainty induces error in the reconstructed displacement [29]. Simulations with additive white noise displacements of different power spectrum density (PSD) were performed to assess the impact of noise and the results are summarized in Table V. (Note that 100 $pm/\sqrt{Hz}$ is a typical PSD value for standard OFI signals whereas significantly lower PSD values of $\sim$ 1 pm/$\sqrt{Hz}$ can be achieved for the FM channel of OFI [12].) Table V shows that when PSD is less than 100 $pm/\sqrt{Hz}$, the obtained performances with ZC are still about 40% better than without,

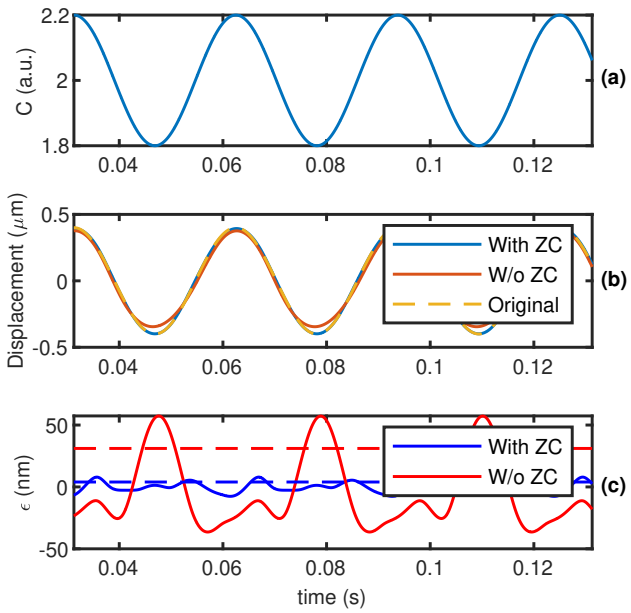

Fig. 8. Simulated results of reconstructing the displacement from an OFI signal corresponding to a harmonic motion with 0.4 μm at 32 Hz with α = 5 and λ_0 = 785 nm such that (a) C is varied by 20% in a sinusoidal manner with a mean value of 2. (b) Comparison of reference target motion (dashed line) with reconstructed displacement with- (blue line) and without-proposed ZC method (red line). (c) Corresponding error in reconstructed displacement ϵ (unbroken line) and its RMS value (dashed line).

TABLE IV

SIMULATED COMPARISON OF RMS ERROR RESULTS OF THE PROPOSED ZC METHOD AND THE SIMPLE NUS METHOD FOR OFI SIGNALS WITH C VARYING SINUSOIDALLY BY 20%. f_t = 32 HZ, λ_0 = 785 NM AND α = 5. A_t AND THE MEAN VALUE OF C, DENOTED AS C_m, ARE VARIED.

A_t (μm)	ϵ_{rms} NUS method (nm)		ϵ_{rms} ZC method (nm)	
	C_m = 2	C_m = 4	C_m = 2	C_m = 4
0.4	33.0	255	8.15	27.7
0.8	16.0	38.2	9.46	26.3
1.2	13.9	29.0	10.1	32.5
5.0	13.4	30.1	15.2	63.6
10	14.3	30.9	10.9	43.6

which can be considered as significant for small displacement amplitudes.

V. EXPERIMENTAL RESULTS

A. Experimental Setup

The proposed ZC method is tested on different experimentally acquired OFI signals to quantify its performance. The testbench shown in Fig. 9 was used to obtain the required signals. Hitachi HL7851G laser diode package was used in the experimental setup, having λ_0 = 785 nm with an output power of 50 mW, and a typical threshold current of 45 mA. Physik Instrumente (P753.2CD) piezoelectric transducer (PZT) was used as the target, which consists of an internal capacitive position sensor with a 0.2 nm resolution and 2 nm repeatability. NI USB 6251 data acquisition system was utilized to acquire data that was sampled at the rate of 5x10^5 samples/s with 16-bits resolution. The laser diode and the PZT were positioned 35 cm apart.

TABLE V

SIMULATION BASED PERFORMANCE AND PERCENTAGE IMPROVEMENT OF THE PROPOSED ZC METHOD IN CASE OF ADDITIVE NOISE AS COMPARED TO THE SIMPLE NUS METHOD. C = 2, α = 5 FOR A TARGET MOTION OF 0.5 μM AMPLITUDE AT 10 HZ WITH λ = 785 NM AND Fs = 1 MHZ.

Amp. (μm)	PSD (pm/$\sqrt{Hz}$)	Accuracy (%)	% Imp.
0.5	0	99.31	87.8
0.5	10	99.30	87.7
0.5	100	98.24	68.5
0.5	200	95.03	17.9
0.5	1000	-125.16	-51.7
1	0	99.49	77.3
1	10	99.46	75.9
1	100	98.62	37.7
1	200	97.99	9.9
1	1000	59.25	26.3

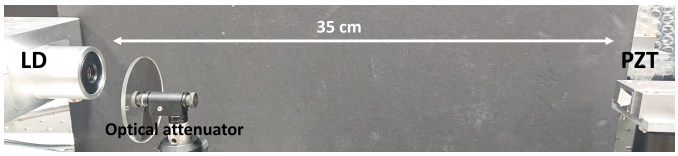

Fig. 9. OFI testbench for experimentation of zero-crossing based NUS approach. Piezoelectric transducer (PZT) containing internal capacitive sensor with 2 nm resolution is used to generate target displacement $D(t)$.

B. Results

The proposed ZC method was tested for two different PZT frequencies i.e., f_t = 10 Hz and f_t = 60 Hz, and at three different amplitude values i.e., A_t = 0.25 μm, A_t = 1 μm, and A_t = 4 μm (see Table VI and Table VII). For every above-mentioned $\{f_t, A_t\}$ case, 5 acquisitions of one-second duration each were saved, and used for the testing of the proposed method. By using the reference PZT measurement, RMS errors were quantified for each one-second long acquisition. Then, using the 5 acquisitions for every $\{f_t, A_t\}$ case, mean and standard deviation (SD) was computed, and reported in Table VI and Table VII for C estimation and measurement error. Same process was repeated by using the simple NUS method without zero-crossings, and corresponding percentage improvement was also calculated. It can be seen from Table VI and Table VII that the proposed method gives improved results in all reported $\{f_t, A_t\}$ cases. It is also apparent that the maximum improvement in measurement precision is obtained when the remote displacement has an amplitude comparable to $\lambda_0/2$, and this finding corroborates with the simulated results of the previous section.

Few specific cases are also discussed here. When the ZC method is applied to an experimental OFI signal corresponding to 0.25 μm amplitude at 10 Hz with $\widehat{\alpha}$ = 5 and $\widehat{C}$ = 1.78 (estimated by using the method reported in [26] with a precision of $< 5\%$), an improvement of 92% in RMS error

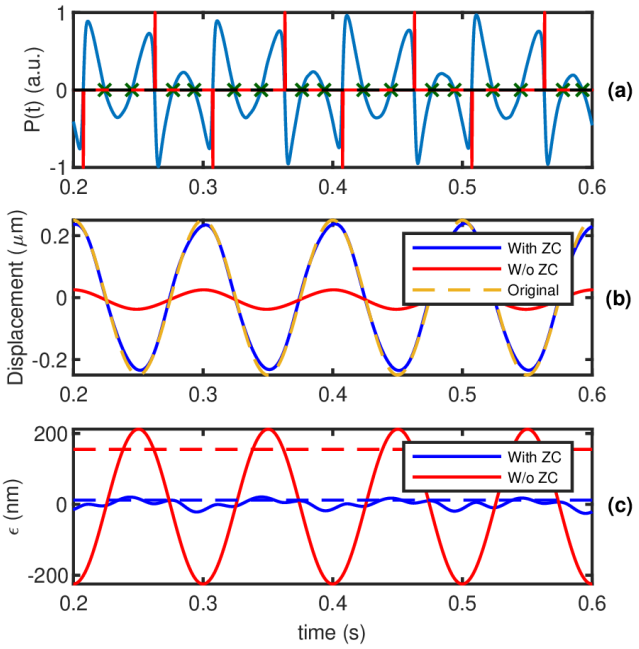

Fig. 10. (a) Detected zero crossings (green crosses) and fringe discontinuities (red vertical lines) on filtered experimental OFI signal obtained for a PZT motion with $\boldsymbol{A_t}$ = 0.25 μm at 10 Hz using HL7851 LD with wavelength $\boldsymbol{\lambda_0}$ = 785 nm, $\widehat{\boldsymbol{C}}$ = 1.78 and $\widehat{\boldsymbol{\alpha}}$ = 5. (b) Comparison of reconstructed signals with- (blue line) and without-ZC method (red line), with reference PZT displacement (orange dashed line), and (c) corresponding error signals and RMS errors (dashed lines) obtained by comparing the reconstructed signals with the reference PZT displacement.

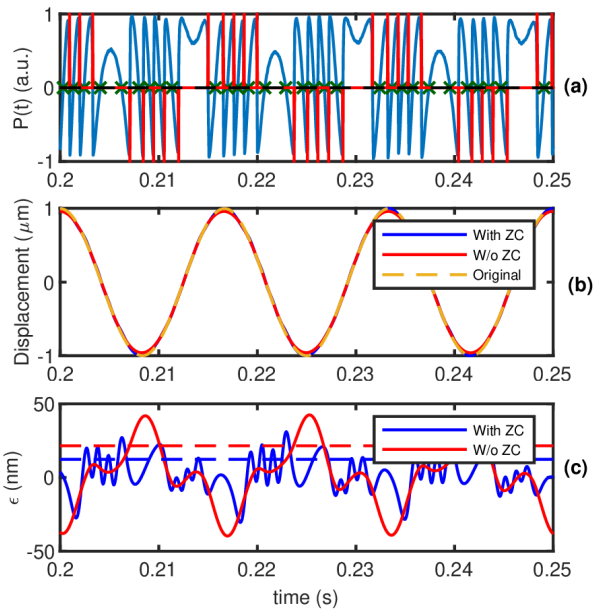

Fig. 11. (a) Detected zero crossings (green markers) and fringe discontinuities (red lines) on filtered experimental OFI signal obtained for a displacement with amplitude $\boldsymbol{A_t}$ = 1 μm at 60 Hz using wavelength $\boldsymbol{\lambda_0}$ = 785 nm, $\widehat{\boldsymbol{C}}$ = 1.78 and $\boldsymbol{\alpha}$ = 5. (b) Comparison of reconstructed signals with ZC method (blue) and without ZC method (red), with reference sinusoidal displacement (orange), and corresponding (c) error signals and RMS errors (dashed lines) obtained by comparing the reconstructed signals with the reference displacement.

is observed (see also Fig. 10). For the given case, the simple NUS method only detects the fringe discontinuities in the OFI signal. On the other hand, the ZC method additionally detects zero-crossings at the 'humps' in the OFI signal (see Fig. 10 (a)) as well, thereby doubling the number of time-phase pairs that results in a better reconstruction of the displacement. The RMS error without ZC method is measured to be about 155 nm, whereas the RMS error with ZC method is around 12 nm (see Fig. 10 (c)).

Similarly, for the OFI signal acquired for $A_t = 1$ μm at 60 Hz (5 fringes per cycle) with $\widehat{C}$ = 1.1838, an improvement of 43% in RMS error was observed for this case (see Fig. 11).

TABLE VI
PERFORMANCE OF THE PROPOSED ZC METHOD ON EXPERIMENTAL OFI SIGNALS FOR PZT FREQUENCY OF 10 HZ AND DIFFERENT AMPLITUDES. 5 ACQUISITIONS OF 1-SECOND DURATION WERE USED FOR EACH CASE.

A_t (μm)	No. of fringes	$\widehat{C}$	S.D. of C	Average ϵ_{rms} (nm)	S.D. (nm)	% Imp.
0.25	1	1.78	0.0	22.4	5.9	85.5
1.00	5	1.04	0.07	38.7	4.5	15.0
4.00	20	1.34	0.02	161.9	0.7	3.9

VI. DISCUSSION

The proposed method provides high measurement precision when the remote target motion is of low amplitudes.

TABLE VII
PERFORMANCE OF THE ZC METHOD ON EXPERIMENTAL OFI SIGNALS FOR PZT FREQUENCY OF 60 HZ AND DIFFERENT $\boldsymbol{A_t}$. 5 ACQUISITIONS OF 1-SECOND DURATION WERE PROCESSED FOR EACH CASE.

A_t (μm)	No. of fringes	$\widehat{C}$	S.D. of C	Average ϵ_{rms} (nm)	S.D. (nm)	% Imp.
0.28	1	1.78	0.0	19.6	7.16	77.8
0.97	5	1.21	0.03	19.9	0.59	33.3
4.00	20	2.39	0.04	77.8	0.4	2.0

However, error in C estimation will result in reconstruction error because of the erroneous calculation of phase difference between zero-crossings and fringe discontinuities. As a result, the improvement provided by the proposed ZC method becomes less relevant than the classical NUS approach whose precision directly benefits in case of increase in the number of crossed quantization levels occurring for higher displacement amplitude. Furthermore, the improvement is constrained by the shape of the OFI signal. Maximum improvement is observed when the so-called hump of the OFI signal cuts across the zero-line, an aspect dependent on C, α and initial phase value (e.g., the abrupt reduction in error observed in Fig. 5 and Fig. 6 (when A_t is around 2 μm) for the proposed method is due to ZCs in the hump zones).

For a given remote motion, laser wavelength, and initial phase value, occurrence of zero-crossings in an OFI signal is a function of C and α (see Fig. 12 (a)). It can be seen that the upward and downward OFI fringes both cross the zero-line

only for certain combinations of $[C\ \alpha]$, shown as the green zone in Fig. 12 (a) obtained for a peak to peak displacement of $4.1\lambda_0$ (so greater than $\lambda_0/2$ to generate fringes). As C increases, due to the hysteresis in OFI signals, only upward fringes cross the zero-line, shown as the blue zone. For further increase in C, neither upward nor downward fringes cross the zero-line, shown as the red zone. For the best performance of the proposed method, $[C\ \alpha]$ combination should be such that all possible zero-crossing points are available, i.e. the operating conditions correspond to the green zone. Then, in case of an increase in C, if the sensor is operating in the blue zone then the proposed method still has zero-crossing points to improve the performance as compared with the simple NUS method. However, in case of strong feedback, it may so happen that there are no more zero-crossings in the OFI signal. This scenario is shown in Fig. 12 (b) where an OFI signal with $C = 9$ and $\alpha = 3$ has no zero-crossings due to high C value. This $[C\ \alpha]$ combination is represented by the yellow oval in Fig. 12 (a). Thus, the improvement provided by the proposed method decreases with increase in C and the performance eventually becomes comparable to the simple NUS method for very strong feedback. However, note that in case of strong optical feedback, phenomenon of fringe-loss [30] also appears which limits the performance of most motion retrieval algorithms. That is why, efforts have been previously made to ensure that the optical feedback strength is controlled to maintain the laser sensing in the moderate feedback regime, such as by using a liquid lens [31].

Note also that the lower detection limit of the proposed ZC method is the same as the NUS method in case of no dithering in either method. One quantization level corresponding to a fringe discontinuity is still required for the proposed ZC method. Without this quantization level, it is not possible to correctly quantify the amplitude of the displacement. But if dithering is done and that the resulting average sampling rate (fringes and ZC) of the input exceeds twice the input signal bandwidth, then the lower limit would be given by the noise-equivalent displacement. The ZC method will provide better reconstruction in the case dithering is performed.

The experimental signals also require precise noise removal filtering. Zero-crossings and fringe discontinuities can be detected incorrectly on noisy signals, and inaccurate detection of a single fringe-discontinuity or zero-crossing can degrade the interpolation. Regardless, the method has shown improvement in reconstruction compared to the simple NUS method over a wide range of C, A_t and f_t values in simulations. Up to 85.5% improvement in RMS error is also reported for experimental signals. Therefore, due to the inherent simplicity of the proposed method and its ability to deal with small amplitudes by doubling the number of samples or events for NUS systems, the proposed method is considered to contribute to this area of sensing and instrumentation.

VII. Conclusions

The zero-crossing based non-uniform sampling method for OFI, proposed in this paper, has enabled higher measurement precision for such a system operating under moderate optical feedback regime.

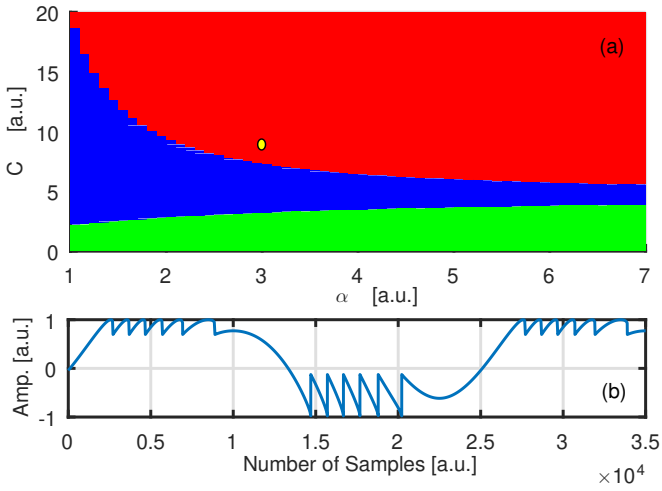

Fig. 12. (a) Occurrence of zero-crossings in an OFI signal as a function of $\boldsymbol{C}$ and $\boldsymbol{\alpha}$ for a peak to peak displacement of $\boldsymbol{4.1\lambda_0}$. Upward and downward fringes both cross the zero-line (green zone), only upward fringes cross the zero-line (blue zone), or neither upward nor downward fringes cross the zero-line (red zone). (b) An OFI signal with $\boldsymbol{C = 9}$ and $\boldsymbol{\alpha = 3}$ in which no ZC occurs due to high $\boldsymbol{C}$ value. This $[\boldsymbol{C\ \alpha}]$ combination is represented by the yellow oval in subplot (a).

Parametric analysis of applying the proposed method shows RMS error improvements of 25% to 95% for low-amplitude motion in the moderate feedback regime compared to the previous dither-less NUS method. Similarly, experimental results indicate an improvement of more than 80% in RMS error. This improved reconstruction is a result of using zero-crossings along with fringe discontinuities of the OFI signal to define the phase quantization levels, which allows for more accurate interpolation around the maxima and minima where the simple NUS method lacks discontinuity points/events. The proposed method thus mitigates the need to add (and later remove) dithering for such low-amplitude motion.

Acknowledgement

The authors would like to thank ANR-20-CE42-0010 PICSONDE in cooperation with ACOEM, Thierry MAZOYER for their support in this project.

References

[1] T. Taimre, M. Nikolić, K. Bertling, Y. L. Lim, T. Bosch, and A. D. Rakić, "Laser feedback interferometry: a tutorial on the self-mixing effect for coherent sensing," *Advances in Optics and Photonics*, vol. 7, no. 3, pp. 570–631, 2015.

[2] A. Valavanis, P. Dean, Y. L. Lim, R. Alhathlool, M. Nikolic, R. Kliese, S. P. Khanna, D. Indjin, S. J. Wilson, A. D. Rakic, *et al.*, "Self-mixing interferometry with terahertz quantum cascade lasers," *IEEE Sensors Journal*, vol. 13, no. 1, pp. 37–43, 2012.

[3] M. Veng, J. Perchoux, and F. Bony, "Fringe disappearance in self-mixing interferometry laser sensors: Model and application to the absolute distance measurement scheme," *IEEE Sensors Journal*, vol. 19, no. 14, pp. 5521–5528, 2019.

[4] O. D. Bernal, U. Zabit, F. Jayat, and T. Bosch, "Sub-λ/2 displacement sensor with nanometric precision based on optical feedback interferometry used as a non-uniform event-based sampling system," *IEEE Sensors Journal*, vol. 20, no. 10, pp. 5195–5203, 2020.

[5] G. Plantier, N. Servagent, T. Bosch, and A. Sourice, "Real-time tracking of time-varying velocity using a self-mixing laser diode," *IEEE transactions on instrumentation and measurement*, vol. 53, no. 1, pp. 109–115, 2004.

[6] C. Wang, X. Li, K. Kou, T. Wu, and H. Xiang, "High resolution quartz flexure accelerometer based on laser self-mixing interferometry," *Review of Scientific Instruments*, vol. 86, no. 6, p. 065001, 2015.

[7] M. Norgia, A. Pesatori, and L. Rovati, "Self-mixing laser doppler spectra of extracorporeal blood flow: a theoretical and experimental study," *IEEE Sensors Journal*, vol. 12, no. 3, pp. 552–557, 2011.

[8] Y. Zhao, J. Zhou, C. Wang, Y. Chen, and L. Lu, "Temperature measurement of the laser cavity based on multi-longitudinal mode laser self-mixing effect," *IEEE Sensors Journal*, vol. 19, no. 12, pp. 4386–4392, 2019.

[9] M. Dabbicco, A. Intermite, and G. Scamarcio, "Laser-self-mixing fiber sensor for integral strain measurement," *Journal of lightwave technology*, vol. 29, no. 3, pp. 335–340, 2011.

[10] N. Ali, U. Zabit, and O. D. Bernal, "Nanometric vibration sensing using spectral processing of laser self-mixing feedback phase," *IEEE Sensors Journal*, vol. 21, no. 16, pp. 17766–17774, 2021.

[11] J. Perchoux, A. Quotb, R. Atashkhooei, F. J. Azcona, E. E. Ramírez-Miquet, O. Bernal, A. Jha, A. Luna-Arriaga, C. Yanez, J. Caum, *et al.*, "Current developments on optical feedback interferometry as an all-optical sensor for biomedical applications," *Sensors*, vol. 16, no. 5, p. 694, 2016.

[12] S. Donati and M. Norgia, "Self-mixing interferometer with a laser diode: unveiling the fm channel and its advantages respect to the am channel," *IEEE Journal of Quantum Electronics*, vol. 53, no. 5, pp. 1–10, 2017.

[13] S. Donati, "Developing self-mixing interferometry for instrumentation and measurements," *Laser & Photonics Reviews*, vol. 6, no. 3, pp. 393–417, 2012.

[14] G. Giuliani, S. Bozzi-Pietra, and S. Donati, "Self-mixing laser diode vibrometer," *Meas. Sci. Technol*, vol. 14, pp. 24–32, 01 2003.

[15] Z. Wei, W. Huang, J. Zhang, X. Wang, H. Zhu, T. An, and X. Yu, "Obtaining scalable fringe precision in self-mixing interference using an even-power fast algorithm," *IEEE photonics journal*, vol. 9, no. 4, pp. 1–11, 2017.

[16] S. Merlo and S. Donati, "Reconstruction of displacement waveforms with a single-channel laser-diode feedback interferometer," *IEEE journal of quantum electronics*, vol. 33, no. 4, pp. 527–531, 1997.

[17] C. Bes, G. Plantier, and T. Bosch, "Displacement measurements using a self-mixing laser diode under moderate feedback," *IEEE Transactions on Instrumentation and Measurement*, vol. 55, no. 4, pp. 1101–1105, 2006.

[18] Y. Fan, Y. Yu, J. Xi, and J. F. Chicharo, "Improving the measurement performance for a self-mixing interferometry-based displacement sensing system," *Applied Optics*, vol. 50, no. 26, pp. 5064–5072, 2011.

[19] O. D. Bernal, U. Zabit, and T. Bosch, "Study of laser feedback phase under self-mixing leading to improved phase unwrapping for vibration sensing," *IEEE Sensors Journal*, vol. 13, no. 12, pp. 4962–4971, 2013.

[20] O. D. Bernal, U. Zabit, T. Niakan, A. Raghubanshi, F. Jayat, and T. Bosch, "Non-uniform sampling theory applied to optical feedback interferometry for displacement sensors," in *2020 IEEE International Instrumentation and Measurement Technology Conference (I2MTC)*, pp. 1–5, IEEE, 2020.

[21] R. Lang and K. Kobayashi, "External optical feedback effects on semiconductor injection laser properties," *IEEE Journal of Quantum Electronics*, vol. 16, no. 3, pp. 347–355, 1980.

[22] G. Acket, D. Lenstra, A. Den Boef, and B. Verbeek, "The influence of feedback intensity on longitudinal mode properties and optical noise in index-guided semiconductor lasers," *IEEE Journal of Quantum Electronics*, vol. 20, no. 10, pp. 1163–1169, 1984.

[23] T. Taimre and A. D. Rakić, "On the nature of acket's characteristic parameter c in semiconductor lasers," *Applied optics*, vol. 53, no. 5, pp. 1001–1006, 2014.

[24] C. Henry, "Theory of the linewidth of semiconductor lasers," *IEEE Journal of Quantum Electronics*, vol. 18, no. 2, pp. 259–264, 1982.

[25] G. Plantier, C. Bes, and T. Bosch, "Behavioral model of a self-mixing laser diode sensor," *IEEE Journal of Quantum Electronics*, vol. 41, no. 9, pp. 1157–1167, 2005.

[26] O. D. Bernal, U. Zabit, F. Jayat, and T. Bosch, "Toward an estimation of the optical feedback factor c on the fly for displacement sensing," *Sensors*, vol. 21, no. 10, p. 3528, 2021.

[27] A. A. Siddiqui, U. Zabit, O. D. Bernal, G. Raja, and T. Bosch, "All analog processing of speckle affected self-mixing interferometric signals," *IEEE Sensors Journal*, vol. 17, no. 18, pp. 5892–5899, 2017.

[28] U. Haider, U. Zabit, and O. D. Bernal, "Variable optical feedback-based behavioral model of a self-mixing laser sensor," *IEEE Sensors Journal*, vol. 21, no. 15, pp. 16568–16575, 2021.

[29] C. Vezyrtzis and Y. Tsividis, "Processing of signals using level-crossing sampling," in *2009 IEEE International Symposium on Circuits and Systems*, pp. 2293–2296, IEEE, 2009.

[30] U. Zabit, F. Bony, T. Bosch, and A. D. Rakic, "A self-mixing displacement sensor with fringe-loss compensation for harmonic vibrations," *IEEE Photonics Technology Letters*, vol. 22, no. 6, pp. 410–412, 2010.

[31] O. D. Bernal, U. Zabit, and T. M. Bosch, "Robust method of stabilization of optical feedback regime by using adaptive optics for a self-mixing micro-interferometer laser displacement sensor," *IEEE Journal of Selected Topics in Quantum Electronics*, vol. 21, no. 4, pp. 336–343, 2014.

Hajira S. Bazaz is currently pursuing a Joint Master's degree in Embedded Computing Systems at TU Kaiserslautern, Germany, and University of Southampton, United Kingdom, as part of an Erasmus Mundus program. She obtained her Undergraduate degree in Electrical Engineering from the National University of Sciences and Technology (NUST), Islamabad, Pakistan in 2022. Her research interests lie in the areas of computer architecture, system-on-chip design, and security of computing systems.

Mohaimen M. Fatimah is a postgraduate student at the University of Southampton, pursuing a Joint Master's degree in Embedded Computing Systems. She earned her Bachelor's degree in Electrical Engineering from National University of Sciences and Technology (NUST), Islamabad, Pakistan in 2022. Her research interests center around embedded processors and high-level synthesis.

Layba Asim is a Process Engineer at Tetra Pak's Lahore Converting Factory in Pakistan. She received her Bachelor's degree in Electrical Engineering from the National University of Sciences and Technology (NUST), Islamabad, Pakistan in 2022. Her research interests include signal processing and optimizing production processes.

Usman Zabit completed his Ph.D. degree from Institut National Polytechnique Toulouse (INPT), Toulouse, France, in 2010. He is currently a Professor at National University of Sciences and Technology (NUST), Islamabad, Pakistan. His research focuses on signal processing for sensing applications.

Olivier D. Bernal (M'03-SM'21) received the M.Sc. degree in electrical engineering and the Ph.D. degree from Institut National Polytechnique Toulouse (INPT), Toulouse, France, in 2003 and 2006, respectively. He joined the OpticAl Sensors and smart Integrated Systems group (OASIS) of the LAAS-CNRS laboratory and INPT in 2009, where he is currently an Assistant Professor. His main research interests include the design of integrated analog circuit design for optoelectronics and space applications as well as the design of optical sensors.